Inorganic Chemistry
Article
pubs.acs.org/IC

# Structurally Diverse Copper Complexes Bearing NNO-Tridentate Schiff-Base Derivatives as Efficient Catalysts for Copolymerization of Carbon Dioxide and Cyclohexene Oxide

Chen-Yen Tsai,[†] Bor-Hunn Huang,[†] Mon-Wei Hsiao,[†] Chu-Chieh Lin,*[,†,‡] and Bao-Tsan Ko*[,†]

[†]Department of Chemistry and [‡]Center of Nanoscience & Nanotechnology, National Chung Hsing University, Taichung 402, Taiwan

Supporting Information

**ABSTRACT:** Structurally diverse copper acetate complexes based on NNO-tridentate Schiff-base ligands were synthesized and characterized as mono-, di-, and trinuclear complexes with respect to varied ancillary ligands. Treatment of the ligand precursors ($\mathbf{L^1}$-H = 2-(1-((2-(dimethylamino)ethyl)imino)ethyl)-4-methylphenol, $\mathbf{L^2}$-H = 4-chloro-2-(1-((2-(dimethylamino)ethyl)imino)ethyl)phenol, and $\mathbf{L^3}$-H = 2-(1-((2-(dimethylamino)ethyl)imino)ethyl)-5-methylphenol) with $Cu(OAc)_2 \cdot H_2O$ (1 equiv) in refluxing ethanol afforded five-coordinate mono- or bimetallic copper complexes ($[(\mathbf{L^1})Cu(OAc)(H_2O)]$ (**1**); $[(\mathbf{L^2})Cu(OAc)(H_2O)]$ (**2**); $[(\mathbf{L^3})_2Cu_2(OAc)_2]$ (**3**)) in high yields. Dinuclear copper acetate analogue $[(\mathbf{L^1})_2Cu_2(OAc)_2]$ (**4**) resulted from treatment of $\mathbf{L^1}$-H as the ligand precursor in refluxing anhydrous MeOH with equimolar proportions of metal acetate salt under a dry nitrogen atmosphere. However, a trinuclear complex, $[(\mathbf{L^4})_2Cu_3(OAc)_4]$ (**5**), was obtained on utilizing 2-(1-((2-(dimethylamino)ethyl)imino)ethyl)-5-methoxyphenol ($\mathbf{L^4}$-H) as the proligand under the same synthetic route of **1**–**3**; this complex was also synthesized in the reaction of $\mathbf{L^4}$-H and copper(II) acetate monohydrate in the ratio of 2:3, giving a quantitative yield. All complexes are active catalysts for copolymerization of cyclohexene oxide (CHO) and $CO_2$ without cocatalysts. In particular, dinuclear Cu complex **3** performed satisfactorily to produce polycarbonates with controllable molecular weights and high carbonate linkages. These copper complexes are the first examples that are effective for both $CO_2$/CHO copolymerization and formation of polymers in a controlled fashion.

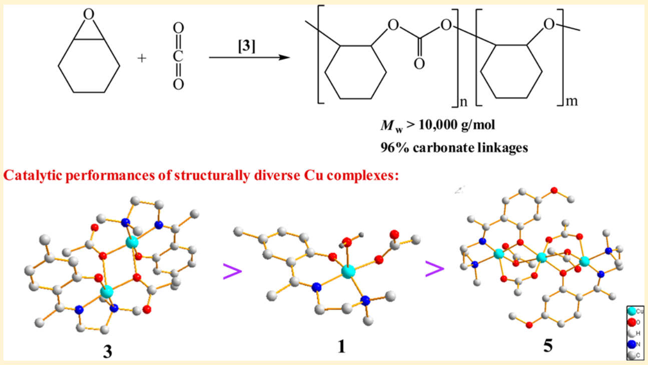

## ■ INTRODUCTION

The catalytic transformation of carbon dioxide ($CO_2$) to fine chemicals has long attracted considerable attention because of its abundant, inexpensive, almost nontoxic, and biorenewable character. Metal-catalyzed epoxide/$CO_2$ alternating copolymerization provides a promising synthetic path to transform $CO_2$ into aliphatic polycarbonates, as shown in Scheme 1a.[1] Various impressive catalytic systems including cobalt, chromium, iron, magnesium, titanium, and zinc complexes bearing various ancillary ligands were therefore developed to perform satisfactorily with high turnover frequencies (TOF) and selectivity of copolymerization.[2] For instance, Williams et al. reported bimetallic Co(II/III),[3] Fe(III),[4] Zn(II),[5] and Mg(II)[6] acetate catalysts in a series incorporating macrocyclic ligands for copolymerization of cyclohexene oxide (CHO) and $CO_2$. The latter dinuclear magnesium complexes displayed outstanding activity even under $CO_2$ at pressure of 1 atm and showed excellent selectivity with high percentage of carbonate linkages.[6] For practical applications, copper(II)-based catalysts seem to be a promising alternative by virtue of their inexpensive nature and insensitivity to air, but most copper complexes give only cyclic carbonates in the $CO_2$/epoxide coupling.[7]

**Scheme 1. Copolymerization of $CO_2$ and Epoxide**

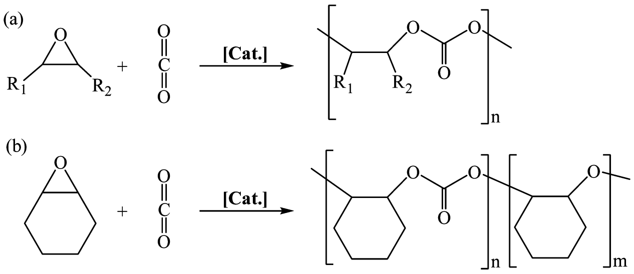

Among ancillary ligand systems employed in catalytic applications, Schiff-base ligands are widely utilized due to easily modifiable steric and electronic effects; magnesium and zinc alkoxides supported by NNO-tridentate Schiff-base derivatives were shown to be excellent initiators for the ring-opening polymerization of lactide.[8] Although mono- and tetranuclear copper acetate complexes based on such Schiff-base ligands have been reported,[9] no bi- or trimetallic copper

**Received:** January 28, 2014
**Published:** May 6, 2014

dx.doi.org/10.1021/ic5002122 | Inorg. Chem. 2014, 53, 5109–5116

Scheme 2. Synthetic Routes of Copper Complexes 1−5

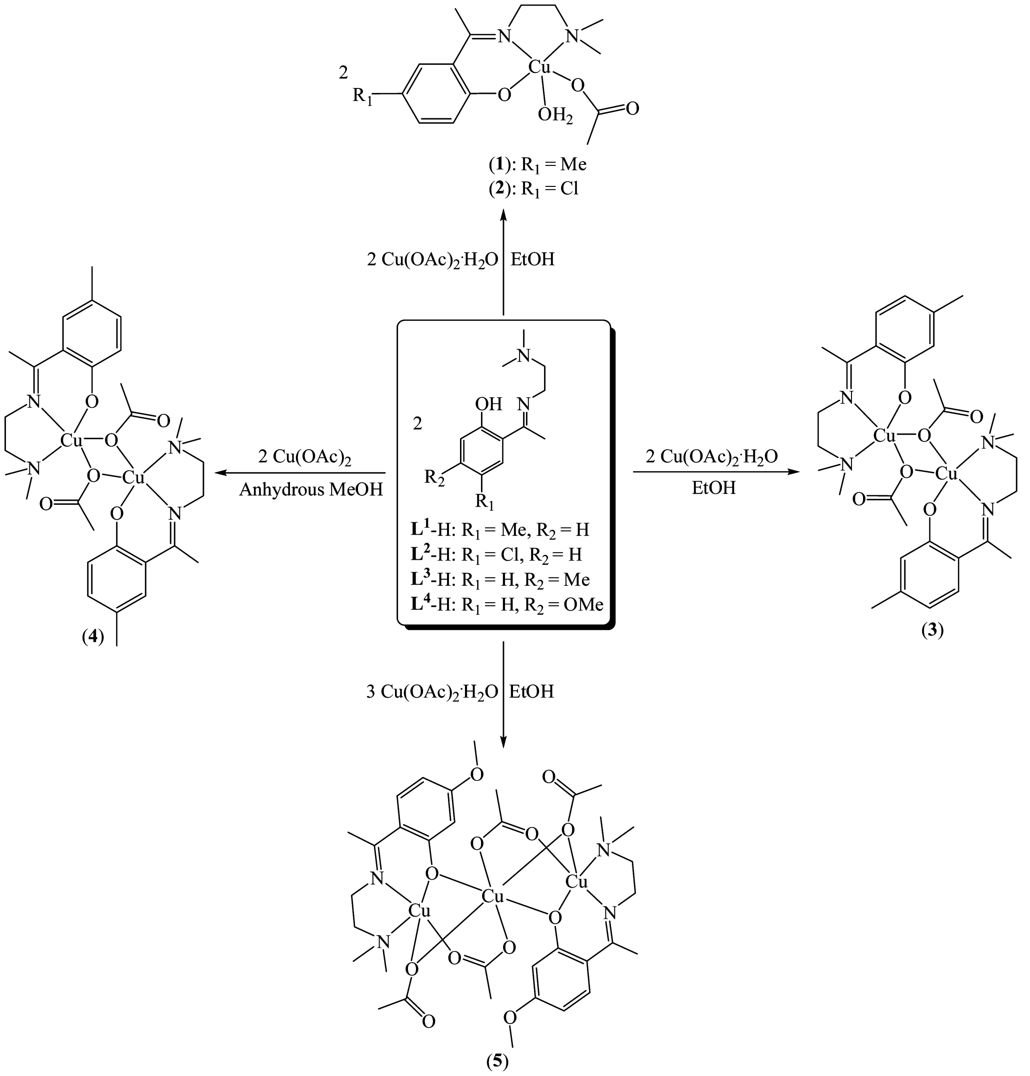

acetate complex of these NNO-tridentate Schiff-base ligands has been isolated. We envisaged that modulating an electronic or steric effect on the substituents might lead to the di- and trinuclear conformations; we hence investigated the catalysis of these complexes in $CO_2$/CHO copolymerization (Scheme 1b). Herein we report for the first time the use of well-defined copper complexes as catalysts to form poly(cyclohexene carbonate).

## ■ RESULTS AND DISCUSSION

**Synthesis and Characterization.** NNO-tridentate Schiff-base proligands were prepared in a series with good yields from meta- or para-substituted 2-hydroxyacetophenone derivatives with *N,N*′-dimethylethane-1,2-diamine in stoichiometric proportions in refluxing ethanol solution.[8b,c] Copper complexes coordinated with NNO-tridentate Schiff-base ligands and acetate (−OAc) groups were readily synthesized via a one-step procedure of copper acetate salt ([$Cu(OAc)_2 \cdot H_2O$]) with the ligand precursors, as illustrated in Scheme 2. Treatment of $Cu(OAc)_2 \cdot H_2O$ with 2-(1-((2-(dimethylamino)ethyl)imino)ethyl)-4-methylphenol (**L**$^1$-H) or 4-chloro-2-(1-((2-(dimethylamino)ethyl)imino)ethyl)phenol (**L**$^2$-H) (1.0 mol equiv) in refluxing ethanol gave monomeric five-coordinate copper complexes [(**L**$^1$)Cu(OAc)($H_2O$)] (**1**) and [(**L**$^2$)Cu(OAc)($H_2O$)] (**2**), but the reaction of 2-(1-((2-(dimethylamino)ethyl)imino)ethyl)-5-methylphenol (**L**$^3$-H) with $Cu(OAc)_2 \cdot H_2O$ (1.0 mol equiv) under the same synthetic conditions produced the bimetallic copper complex [$(\mathbf{L}^3)_2Cu_2(OAc)_2$] (**3**) in high yield. Interestingly, $Cu(OAc)_2$ reacted with **L**$^1$-H in equimolar proportions in refluxing anhydrous MeOH to furnish the dinuclear copper acetate analogue [$(\mathbf{L}^1)_2Cu_2(OAc)_2$] (**4**) in good yield. However, a trinuclear complex, [$(\mathbf{L}^4)_2Cu_3(OAc)_4$] (**5**), resulted from treatment of 2-(1-((2-(dimethylamino)ethyl)imino)ethyl)-5-methoxyphenol (**L**$^4$-H) as the proligand according to the same synthetic route of **1**−**3** with a ligand/metal precursor ratio of 1:1. Alternatively, complex **5** was prepared in quantitative yield from the reaction of **L**$^4$-H and copper(II) acetate monohydrate with a ratio of 2:3. All complexes were obtained as air-stable crystalline solids and were characterized on the basis of mass, IR, and ultraviolet−visible (UV−vis) spectra as well as elemental analysis. On the basis of electrospray ionization (ESI) mass spectrum, a daughter peak related to [$(\mathbf{L}^1)Cu]^+$ ($m/z = 282.1$, 100%) was observed in **1**. However, **4** displayed a main peak corresponding to [$(\mathbf{L}^1)_2Cu_2(OAc)]^+$ ($m/z = 623.2$, 100%), indicating Cu complex **4** is dinuclear in solution. The IR spectra displayed two sets of acetate groups in

**5**: carbonyl-stretching bands at 1589 and 1426 $cm^{-1}$ belong to bridging bidentate acetate coordination modes, whereas strong bands at 1526 and 1396 $cm^{-1}$ are attributed to bridging monodentate bound-acetate anion.[10] On the basis of the absorption spectra, the bands in the ranges of 280−330 and 350−400 nm might be assigned to the $\pi-\pi^*$ and $n-\pi^*$ transitions. A broad band from 550 to 650 nm can be ascribed to the d−d transition band, which is typical for a Schiff-base Cu(II) complex (Supporting Information, Figures S1 and S2).[11] Molecular structures of all Cu complexes were confirmed by single-crystal X-ray crystallography.

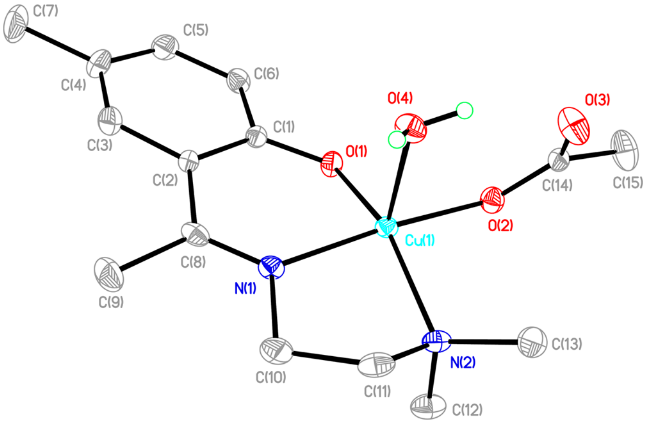

**Figure 1.** ORTEP drawing of complex **1** with probability ellipsoids drawn at 50% level. Hydrogen atoms except for those in O(4) are omitted for clarity. Selected bond lengths (Å) and angles (deg): Cu(1)−O(1) 1.9218(17), Cu(1)−O(2) 1.9660(19), Cu(1)−N(1) 1.979(2), Cu(1)−N(2) 2.048(2), Cu(1)−O(4) 2.2591(17), O(1)−Cu(1)−O(2) 87.46(8), O(1)−Cu(1)−N(1) 90.76(8), O(2)−Cu(1)−N(1) 172.30(8), O(1)−Cu(1)−N(2) 155.10(8), O(2)−Cu(1)−N(2) 3.42(9), N(1)−Cu(1)−N(2) 85.05(9), O(1)−Cu(1)−O(4) 105.37(7), O(2)−Cu(1)−O(4) 94.51(7), N(1)−Cu(1)−O(4) 93.19(7), N(2)−Cu(1)−O(4) 99.37(7).

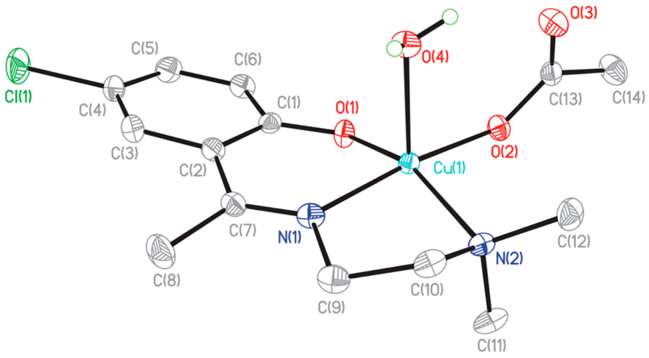

**Figure 2.** ORTEP drawing of complex **2** with probability ellipsoids drawn at 50% level. Hydrogen atoms except for those in O(4) are omitted for clarity. Selected bond lengths (Å) and angles (deg): Cu(1)−O(1) 1.9236(16), Cu(1)−O(2) 1.9516(16), Cu(1)−N(1) 1.982(2), Cu(1)−N(2) 2.0441(19), Cu(1)−O(4) 2.2683(17), O(1)−Cu(1)−O(2) 87.30(7), O(1)−Cu(1)−N(1) 90.38(7), O(2)−Cu(1)−N(1) 171.63(8), O(1)−Cu(1)−N(2) 155.82(8), O(2)−Cu(1)−N(2) 93.33(7), N(1)−Cu(1)−N(2) 85.50(8), O(1)−Cu(1)−O(4) 103.16(7), O(2)−Cu(1)−O(4) 95.11(7), N(1)−Cu(1)−O(4) 93.25(8), N(2)−Cu(1)−O(4) 100.86(7).

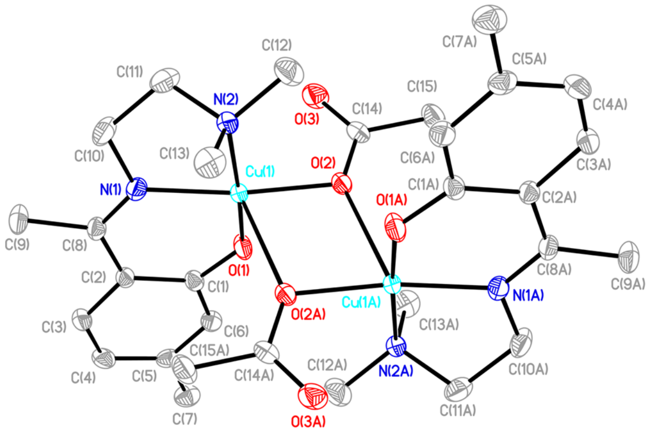

**Figure 3.** ORTEP drawing of complex **3** with probability ellipsoids drawn at 50% level. Hydrogen atoms are omitted for clarity. Selected bond lengths (Å) and angles (deg): Cu(1)−O(1) 1.894(2), Cu(1)−O(2) 1.9776(18), Cu(1)−N(1) 1.965(2), Cu(1)−N(2) 2.063(2), Cu(1)−O(2A) 2.505(2), O(1)−Cu(1)−O(2) 90.11(8), O(1)−Cu(1)−N(1) 91.69(9), O(2)−Cu(1)−N(1) 171.83(11), O(1)−Cu(1)−N(2) 174.59(8), O(2)−Cu(1)−N(2) 93.15(8), N(1)−Cu(1)−N(2) 84.48(9).

**Crystal Structures of Complexes 1−5.** Single crystals of complexes **1**−**5** suitable for X-ray structural determination were grown from their saturated solutions in ethanol or methanol. As shown in Figures 1 and 2, the geometries around the copper centers of five-coordinate complexes **1** and **2** are both distorted square pyramids ($\tau$ = 0.29 for **1** and 0.26 for **2**)[12] constructed by one O and two N atoms of the NNO-tridentate ligand, one O atom from an acetate group, and a coordinated water. The lengths of bonds between the Cu and O(1), O(2), N(1), N(2), and O(4) atoms are 1.9218(17), 1.9660(19), 1.979(2), 2.048(2), and 2.2591(17) Å for **1** and 1.9236(16), 1.9516(16), 1.982(2), 2.0441(19), and 2.2683(17) Å for **2**; all these distances are within the normal ranges reported in the literature.[9] As a result, the electronic effect of substituents at the para position of the phenoxy group seems to be not obvious. The molecular structure of **3**, presented in Figure 3, is a dimeric and pentacoordinate copper complex containing a Cu(1)/O(2)/Cu(1A)/O(2A) planar core with inversion symmetry in which the Cu atom is located ca. 0.1029 Å above the O(1)/O(2)/N(1)/N(2) plane. The geometry around each Cu atom displays a slightly distorted square pyramid ($\tau$ = 0.05)[12] formed by O(1), N(1), and N(2) of an ancillary ligand and two $\mu_2$-acetate oxygen atoms. The bond distances around the Cu atoms for **3** are comparable to those observed in complex **1**, as listed in Table 1. The crystal structure of copper complex **4** (Figure 4) is isostructural with Cu analogue **3**, except that a methyl ($-CH_3$) substituent is at the para position of the phenoxy group. As expected, the average bond lengths of Cu−O(phenoxy) = 1.894(2) Å, Cu−N(imine) = 1.970(3) Å, and Cu−O(OAc) = 2.242(2) Å in **4** are similar to those found for complex **3**, as shown in Table 1. It is noteworthy that the solid-state structures of the mono- and dinuclear complexes **1** and **4** are consistent with the results of their ESI mass spectra.

The Oak Ridge thermal-ellipsoid plot (ORTEP) in Figure 5 shows that two distinct environments of Cu centers constitute the linear trinuclear complex **5** with respect to one hexacoordinate Cu(2) and two pentacoordinate Cu(1) and Cu(1A). Few trinuclear copper acetate complexes are reported.[13] The Cu(2) center exhibits a distorted octahedral geometry formed by two O atoms from two different NNO−backbones, two O atoms from two bridged OAc groups, and two different $\mu_2$-acetate oxygen atoms; a $C_2$ symmetry axis

Table 1. Selected Bond Lengths (Å) for Complexes 1−5

| | 1 | 2 | 3 | 4 | 5 |
|---|---|---|---|---|---|
| Cu(1)−$O_{phenoxy}$ | 1.9218(17) | 1.9236(16) | 1.894(2) | 1.894(2) | 1.956(2) |
| Cu(1)−N(1) | 1.979(2) | 1.982(2) | 1.965(2) | 1.970(3) | 1.960(2) |
| Cu(1)−N(2) | 2.048(2) | 2.0441(19) | 2.063(2) | 2.073(3) | 2.055(3) |
| Cu(1)−$O_{H2O}$ | 2.2591(17) | 2.2683(17) | | | |
| Cu(1)−$O_{monodentate\ OAc}$ | 1.9660(19) | 1.9516(16) | | | |
| Cu(1)−$O_{bridging\ monodentate\ OAc}$ | | | 1.9776(18) | 1.982(2) | 1.956(2) |
| Cu(1A)−$O_{bridging\ monodentate\ OAc}$ | | | 2.505(2) | 2.502(2) | |
| Cu(1)−$O_{bridging\ bidentate\ OAc}$ | | | | | 2.255(2) |
| Cu(2)−$O_{bridging\ monodentate\ OAc}$ | | | | | 2.490(2) |
| Cu(2)−$O_{bridging\ bidentate\ OAc}$ | | | | | 1.936(2) |

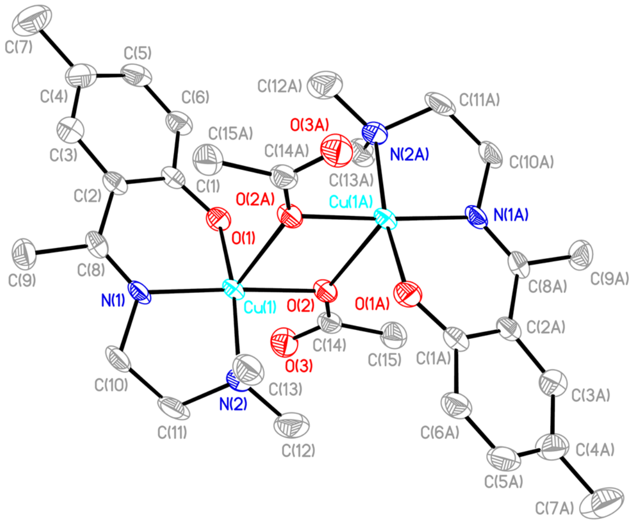

**Figure 4.** ORTEP drawing of complex **4** with probability ellipsoids drawn at 50% level. Hydrogen atoms are omitted for clarity. Selected bond lengths (Å) and angles (deg): Cu(1)−O(1) 1.894(2), Cu(1)−O(2) 1.982(2), Cu(1)−N(1) 1.970(3), Cu(1)−N(2) 2.073(3), Cu(1)−O(2A) 2.502(2), O(1)−Cu(1)−O(2) 91.74(10), O(1)−Cu(1)−N(1) 90.96(11), O(1)−Cu(1)−N(2) 170.18(11), O(2)−Cu(1)−N(1) 177.05(9), O(2)−Cu(1)−N(2) 92.93(10), N(1)−Cu(1)−N(2) 84.22(11).

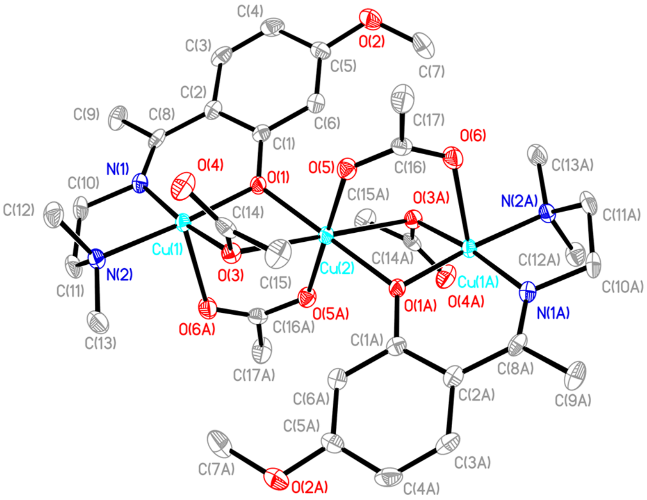

**Figure 5.** ORTEP drawing of complex **5** with probability ellipsoids drawn at 50% level. Hydrogen atoms are omitted for clarity. Selected bond lengths (Å) and angles (deg): Cu(1)−O(1) 1.956(2), Cu(1)−O(3) 1.956(2), Cu(1)−N(1) 1.960(3), Cu(1)−N(2) 2.055(3), Cu(1)-O(6A) 2.255(3), Cu(2)−O(3) 2.490(2), Cu(2)−O(5) 1.936(2), Cu(2)−O(1) 2.019(2), O(3)−Cu(1)−O(1) 87.10(9), O(3)−Cu(1)−N(1) 171.78(10), O(1)−Cu(1)−N(1) 90.03(10), O(3)−Cu(1)−N(2) 98.78(10), O(1)−Cu(1)−N(2) 174.04(10), N(1)−Cu(1)−N(2) 84.01(11), O(3)−Cu(1)−O(6A) 89.09(9), O(1)−Cu(1)−N(6A) 90.23(9), N(1)−Cu(1)−O(6A) 98.64(10), N(2)−Cu(1)−O(6A) 90.78(10), O(5A)−Cu(2)−O(1) 89.07(9), O(5)−Cu(2)−O(1) 90.93(9).

passes through that center. The geometry around pentacoordinated Cu(1) and Cu(1A) is a slightly distorted square pyramid ($\tau$ = 0.04)[12] in which both copper atoms are ca. 0.071 Å above the mean base plane of the pertinent square pyramid. The bond distances between Cu(2) and its neighboring oxygen atoms are all within the normal range reported for six-coordinate copper acetate complexes bearing the NNO-tridentate Schiff-base ligand.[13] In comparison, the five-coordinate Cu-involving bond with Cu(1)−O(1) = 1.956(2) Å is longer than those in complexes **1** and **2**, which is attributed to the phenoxy oxygen atoms bridged to two copper atoms. Four ancillary acetate groups in complex **5** adopt both bridging monodentate and bridging bidentate bonding modes to coordinate the metal center(s) in the solid state, which is consistent with the observations of the IR spectra.

**Copolymerization of Cyclohexene Oxide (CHO) with Carbon Dioxide ($CO_2$).** Copper complexes **1**−**5** were performed to catalyze the coupling of $CO_2$/CHO; representative results appear in Table 2. When the reaction temperature was set at 100 °C (entry 1), the conversion of copolymerization catalyzed with **1** was low (<20%). On raising the temperature to 120 °C with $pCO_2^0$ = 300 psi (entry 2), the TOF increased from 3.75 to 9.38 $h^{-1}$, and a narrowly dispersed copolymer (polydispersity index (PDI) = 1.19) with low molecular weight was obtained. Increasing the concentration of catalyst **1** induced a larger CHO conversion (74%), but the PDI broadened to 1.40 (entry 3). Adjusting the initial pressure of $CO_2$ also affected the $CO_2$/CHO copolymerization (entries 4−5): a higher (500 psi) or lower (100 psi) pressure decreased the TOF and selectivity of copolymerization. However, increasing the duration of reaction also slightly decreased the TOF and broadened the molecular weight distribution (Table 2, entry 6 vs 2). Under the optimal conditions ($[CHO]_0/[catalyst]_0$ = 500/1, $pCO_2^0$ = 300 psi, 120 °C) evaluated from complex **1**, bimetallic Cu complexes **3** and **4** displayed high productivity (CHO conversion = 88%, TON = 440) (TON = number of moles of CHO consumed per mole of catalyst) for 48 h among complexes **1**−**5**, compared with entries 6−10 in Table 2. The selectivities (Supporting Information, Figure S3) and control of molecular weights of the copolymers with Cu catalyst **3** are superior to those of other Cu catalysts in this work, and a copolymer resulted with the higher molecular-weight copoly-

Table 2. Copolymerization of CHO and $CO_2$ Catalyzed by Using Cu Complexes 1−5

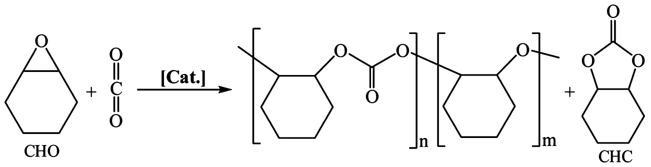

| entry | catalyst[a] (mol %) | time (h) | % CHO conv.[b] | % CHC[b] | % copolymer (% carbonate)[b] | TON[c] | TOF ($h^{-1}$)[d] | $M_n$ (calcd.)[e] | $M_n$ (obsd.)[f] (PDI)[f] |
|---|---|---|---|---|---|---|---|---|---|
| 1[g] | **1**(0.2) | 24 | 18 | 29(trans) | 71(97) | 90 | 3.75 | 9100 | |
| 2 | **1**(0.2) | 24 | 45 | 34(trans) | 66(97) | 225 | 9.38 | 21 100 | 4800(1.19) |
| 3[h] | **1**(0.4) | 24 | 74 | 20(trans) | 80(94) | 185 | 7.71 | 21 000 | 4700(1.40) |
| 4[I] | **1**(0.2) | 24 | 16 | 59(trans) | 41(81) | 80 | 3.33 | 4700 | |
| 5[j] | **1**(0.2) | 24 | 33 | 35(trans) | 65(95) | 165 | 6.88 | 15 200 | 3200(1.29) |
| 6 | **1**(0.2) | 48 | 55 | 20(trans) | 80(96) | 275 | 5.73 | 31 300 | 4900(1.40) |
| 7 | **2**(0.2) | 48 | 25 | 48(trans) | 52(89) | 125 | 2.60 | 9200 | 1900(1.54) |
| 8 | **3**(0.2) | 48 | 88 | 16(trans) | 84(96) | 440 | 9.17 | 26 300 | 9100(1.42) |
| 9 | **4**(0.2) | 48 | 88 | 17(trans) | 83(97) | 440 | 9.17 | 26 300 | 6800(1.56) |
| 10 | **5**(0.2) | 48 | 24 | 19(trans) | 81(38) | 120 | 2.50 | 3500 | |
| 11 | **3**(0.2) | 12 | 45 | 29(trans) | 71(95) | 225 | 18.8 | 11 300 | 3400(1.31) |
| 12 | **3**(0.2) | 24 | 63 | 22(trans) | 78(96) | 315 | 13.1 | 17 500 | 5600(1.46) |
| 13 | **3**(0.2) | 36 | 83 | 16(trans) | 84(96) | 415 | 11.5 | 24 800 | 7000(1.42) |

[a] Copolymerization conditions: CHO 5.0 mL, 0.1 mmol of catalyst, $pCO_2^0$ = 300 psi, $T$ = 120 °C. [b] Determined by comparison of the integrals of signals arising from the methylene protons in the $^1$H NMR spectra, including PCHC carbonate ($\delta$ = 4.65 ppm), PCHC ether ($\delta$ = 3.3−3.5 ppm), and CHC ($\delta$ = 3.9 (trans) or 4.63 ppm (cis)).[4] [c] TON = number of moles of CHO consumed per mole of catalyst. [d] TOF = TON per hour. [e] $[M_w(CHO + CO_2)]$ (142.06 g/mol) times $[CHO]_0/n[catalyst]_0$ times conversion yield times % copolymer ($n$ = 1 for complexes **1** and **2**; $n$ = 2 for complexes **3** and **4**; $n$ = 4 for complex **5**). [f] Determined in THF by GPC. [g] $T$ = 100 °C. [h] 2.5 mL of CHO, 0.1 mmol catalyst. [I] $pCO_2^0$ = 100 psi. [j] $pCO_2^0$ = 500 psi.

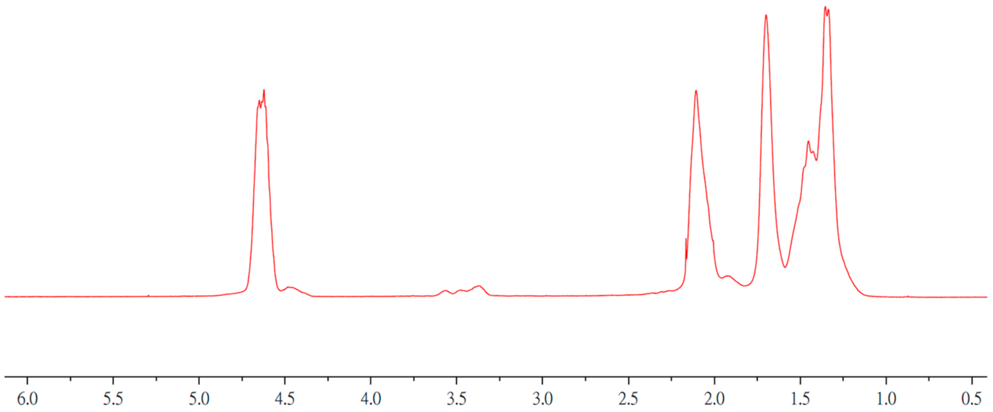

Figure 6. $^1$H NMR spectrum of the purified copolymer produced by using copper acetate complex **3** (Table 2, entry 8) in $CDCl_3$.

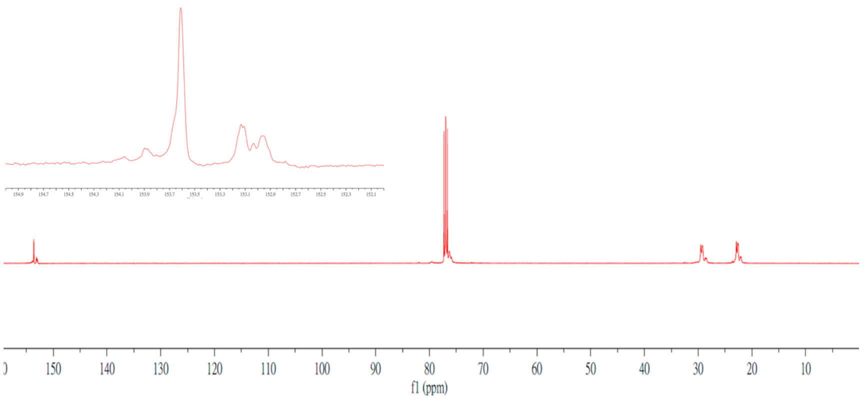

Figure 7. A typical $^{13}$C NMR spectrum of the resultant copolymer (Table 2, entry 8) in $CDCl_3$. (inset) Expanded carbonyl region.

mer ($M_w$ > 10 000 g/mol). Despite the moderate selectivity of the copolymers (copolymer/CHC = 84/16) of CHO/$CO_2$ coupling with **3**, the constituents of carbonate linkages in the polymeric product have a high content (96%). As shown in

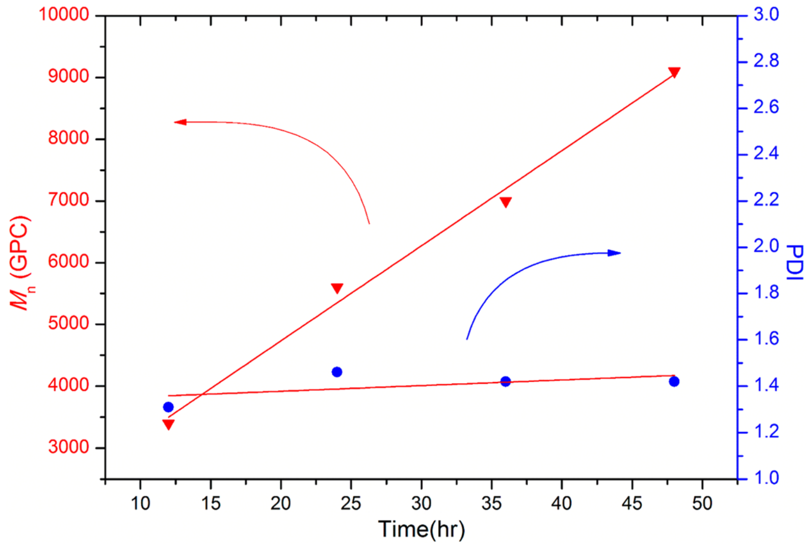

**Figure 8.** Relationship of $M_n$ (▼) and PDI (●) (determined from GPC analysis) vs time for the copolymerization of cyclohexene oxide and $CO_2$ by using dicopper acetate complex **3**.

Figure 6, the $^1$H NMR signal at 4.65 ppm is assigned to the methine protons in the carbonate linkages; the broad signals at 3.3−3.4 ppm correspond to the 4% of ether linkages in the copolymer. Nevertheless, the copolymer produced was almost atactic, based on the $^{13}$C NMR spectrum illustrated in Figure 7. It is noteworthy that the observed molecular weight ($M_n$(GPC)) is significantly lower than the theoretical value based on the acetate anion(s). This can be attributed to the presence of water or alcohol of coordination or crystallization in the catalyst and a small amount of water from the CHO monomer. Trace quantities of protic species that are present in the catalytic system will behave as the chain-transfer agent, resulting in lower molecular weight in comparison with the calculated molecular weight.[14] The superior catalytic performance of dicopper complex **3** might result from a cooperative ring-opening copolymerization via a bimetallic mechanism.[2j,15] The controllable character of **3** was further demonstrated with kinetic experiments that involved variation of $M_n$(GPC) and the molecular weight distribution (PDI) with various durations, as depicted in entries 11−13 of Table 2. A proportional relationship (Figure 8) between $M_n$(GPC) and time for four parallel reactions, along with the remaining narrow PDI (<1.50), implied a controllable copolymerization by dicopper acetate catalyst **3**. To test catalytic activity of these bimetallic copper complexes in copolymerization of propylene oxide (PO) and $CO_2$, coupling of $CO_2$/PO catalyzed by complex **3** was performed under the conditions of 50 °C and 150 psi initial $CO_2$ pressure for 24 h. However, almost negligible PO conversion (<5%) was observed by $^1$H NMR spectrum, and this result indicates that complex **3** is an inactive catalyst for copolymerization of PO and $CO_2$. Although the best catalytic activity of CHO/$CO_2$ copolymerization is only moderate (TOF = 18.8 h$^{-1}$), the results presented here are the first examples to produce copolymers with controllable molecular weights and high carbonate linkages through the use of a bimetallic copper(II) acetate complex containing NNO-tridentate Schiff-base ligands. The theoretical investigation of the mechanism of copper-catalyzed CHO/$CO_2$ copolymerization is in progress.

## ■ CONCLUSIONS

Five diverse copper complexes containing mono-, di-, and trinuclear configurations that depend on the nature of the NNO-tridentate Schiff-base ligands or the conditions of moisture in the environment have been synthesized and fully characterized by X-ray single-crystal structural analyses. The molecular structures differ in the solid state under varied synthetic conditions with treatment of **L$^1$**-H with copper acetate salt in equimolar proportions. Monomeric copper complex **1** containing one coordinated water was formed in a highly moist environment, whereas a dry nitrogen atmosphere afforded dinuclear complex **4** that is a dimeric species containing $Cu_2O_2$ core bridging through monodentate acetate groups. Tri-Cu complex **5** is a rare solid-state example in which four ancillary acetate groups assume both bridging monodentate and bridging bidentate bonding modes to coordinate metal center(s). Bimetallic Cu complex **3** effectively copolymerized $CO_2$ with CHO in a controlled manner; the copolymers were obtained with controllable molecular weights and a high alternating microstructure up to 96% carbonate linkages. Improvement of the catalytic activity of copolymerization utilizing dicopper catalyst **3** in the presence of cocatalysts is under investigation.

## ■ EXPERIMENTAL SECTION

**General Considerations.** Solvents and reagents were dried by refluxing for at least 24 h over sodium/benzophenone (hexane, toluene, tetrahydrofuran (THF)), over phosphorus pentoxide ($CH_2Cl_2$), or over calcium hydride (methanol (MeOH)). Deuterated solvents were dried over 4 Å molecular sieves. $Cu(OAc)_2{\cdot}H_2O$, ethanol (EtOH, 95%), 1-(2-hydroxy-5-methylphenyl)ethanone, 1-(5-chloro-2-hydroxyphenyl)ethanone, 1-(2-hydroxy-4-methylphenyl)-ethanone, 1-(2-hydroxy-4-methoxyphenyl)ethanone, and *N*,*N*′-dimethylethane-1,2-diamine were purchased and used without further purification. Cyclohexene oxide (CHO) was purified before use. $^1$H NMR and $^{13}$C NMR spectra were recorded on Varian Mercury 400 (400 MHz for $^1$H and 100 MHz for $^{13}$C) spectrometer with chemical shifts given in parts per million from the peak of internal tetramethylsilane. Gel permeation chromatography (GPC) measurements were performed on a Jasco PU-2080 plus system equipped with a RI-2031 detector using THF (high-performance liquid chromatography grade) as an eluent (flow rate 1.0 mL/min, at 40 °C). The chromatographic column was Phenomenex Phenogel 5 $\mu$m 103 Å, and the calibration curve used to calculate $M_n$(GPC) was produced from polystyrene standards. The GPC results were calculated using the Scientific Information Service Corporation (SISC) chromatography data solution 3.1 edition. The Fourier transform IR (FT-IR) spectra were recorded on a PerkinElmer Spectrum 100 FT-IR spectrometer in the range of 4000−600 cm$^{-1}$. UV−vis spectra were determined by JASCO U-530 UV−vis spectrometer at 25 °C using $CH_2Cl_2$ as solvent. Mass analyses were performed using positive electron spray ionization (ESI+ or APCI+) technique on a Thermo Finnigan TSQ Quantum mass spectrometer for all these complexes upon dissolving in dimethyl sulfoxide (DMSO) solvent.

**Synthesis of NNO-Schiff-Base Proligands.** General procedures for ligand precursor preparation were conducted by the reaction of corresponding 2-hydroxyacetophenone (5.0 mmol) with *N*,*N*-dimethylethane-1,2-diamine (5.1 mmol) in refluxing ethanol (30.0 mL) for 24 h. The mixture was cooled to room temperature, and the volatile components were removed *in vacuo* to give the products.[16]

*2-(1-((2-(Dimethylamino)ethyl)imino)ethyl)-4-methylphenol* (**$L^1$-H**). Yield: 0.91 g (85%). $^1$H NMR ($CDCl_3$, 400 MHz, ppm): $\delta$ 16.02 (1H, s, −O*H*), 7.29 (1H, d, Ar-*H*), 7.08 (1H, dd, Ar-*H*), 6.82 (1H, d, Ar-*H*), 3.66 (2H, t, $-C{=}N-CH_2-$), 2.71(2H, t, $-CH_2-N(CH_3)_2$), 2.34(6H, s, $-N(CH_3)_2$), 2.33 (3H, s, Ph−$CH_3$), 2.27 (3H, s, $-N{=}C-CH_3$). $^{13}$C NMR ($CDCl_3$, 100 MHz, ppm): $\delta$ 171.6, 161.5, 133.3, 127.9, 125.8, 118.9, 118.4, 59.7, 48.0, 45.8, 20.7, 14.5.

*4-Chloro-2-(1-((2-(dimethylamino)ethyl)imino)ethyl)phenol* (**$L^2$-H**). Yield: 0.99 g (83%). $^1$H NMR ($CDCl_3$, 400 MHz, ppm): $\delta$ 16.41(1H, s,−O*H*), 7.38(1H, d, Ar-*H*), 7.16 (1H, dd, Ar-*H*), 6.80(1H, d, Ar-*H*), 3.60 (2H, t, $-C{=}N-CH_2-$), 2.64 (2H, t, $-CH_2-N(CH_3)_2$), 2.27 (9H, s, $-CH_3$). $^{13}$C NMR ($CDCl_3$, 100 MHz, ppm): $\delta$ 171.0, 163.3, 132.3, 127.2, 120.9, 120.5, 119.4, 59.2, 47.4, 45.6, 14.4.

*2-(1-((2-(Dimethylamino)ethyl)imino)ethyl)-5-methylphenol* (**$L^3$-H**). Yield: 0.93 g (85%). $^1$H NMR ($CD_3Cl$, 400 MHz, ppm): $\delta$ 16.34 (1H, s, −O*H*), 7.38 (1H, d, Ar-*H*), 6.72 (1H, s, Ar-*H*), 6.55 (1H, d, Ar-*H*), 3.30 (2H, t, $-C{=}N-CH_2$-), 2.71 (2H, t, $-CH_2-N(CH_3)_2$), 2.34 (6H, s, $-N(CH_3)_2$), 2.24 (3H, s, $-C{=}N-CH_3$), 2.17 (3H, s, Ar−$CH_3$). $^{13}$C NMR ($CDCl_3$, 100 MHz, ppm): $\delta$ 171.40, 161.5, 133.0, 127.6, 125.2, 118.4, 118.1, 59.2, 47.3, 47.4, 20.3, 14.0.

*2-(1-((2-(Dimethylamino)ethyl)imino)ethyl)-5-methoxyphenol* (**$L^4$-H**). Yield: 0.92 g (78%). $^1$H NMR ($CDCl_3$, 400 MHz, ppm): $\delta$ 16.88 (1H, s, −O*H*), 7.33(1H, d, Ar-*H*), 6.31(1H, d, Ar-*H*), 6.19(1H, dd, Ar-*H*), 3.76(3H, s, $-O(CH_3)$), 3.60(2H, t, $-C{=}N-CH_2-$), 2.65(2H, t, $-CH_2-N(CH_3)_2$), 2.33(3H, s, $-C{=}N-CH_3$), 2.29(6H, s, $-N(CH_3)_2$). $^{13}$C NMR ($CDCl_3$, 100 MHz, ppm): $\delta$ 171.0, 157.6, 150.6, 124.0, 118.9, 113.2, 112.3, 59.5, 55.8, 48.0, 45.6, 14.4.

**Synthesis of Copper Complexes 1−5.** *Synthesis of Complex [[($L^1$)Cu(OAc)($H_2O$)] (1).* A mixture of 2-{1-[2-(dimethylamino)ethyl)-imino]ethyl}-4-methylphenol (1.12 g, 5.1 mmol) and $Cu(OAc)_2{\cdot}H_2O$ (0.995 g, 5.0 mmol) was dissolved in ethanol (30 mL), and the solution was heated under reflux for 24 h. The solution was then cooled to room temperature. Volatile materials were removed to leave about 10 mL under vacuum to yield blue solids. The blue powder was obtained after filtration. Yield: 1.49 g (83%). Anal. Calcd for $C_{15}H_{24}CuN_2O_4$: N, 7.78; C, 50.06; H, 6.72%. Found: N, 7.68; C, 50.34; H, 6.97%. *m*/*z* (ESI-MS, DMSO): 282.1 ($[M-CH_3COO-H_2O]^+$, 100%, calcd. 282.08). Characteristic IR absorptions (cm$^{-1}$, neat): 1615 ($\nu_{C=N}$), 1533 ($\nu_{\text{asymmetric acetate}}$), 1393 ($\nu_{\text{symmetric acetate}}$).

*Synthesis of Complex [($L^2$)Cu(OAc)($H_2O$)] (2).* The synthetic route for complex **2** was the same as that of **1**. Yield: 1.61 g (85%). Anal. Calcd for $C_{14}H_{23}ClCuN_2O_5{\cdot}H_2O$: N, 7.03; C, 42.21; H, 5.82%. Found: N, 6.94; C, 41.66; H, 5.99%. Characteristic IR absorptions (cm$^{-1}$, neat): 1602 ($\nu_{C=N}$), 1522 ($\nu_{\text{asymmetric acetate}}$), 1403 ($\nu_{\text{symmetric acetate}}$).

*Synthesis of Complex [($L^3$)$_2$Cu$_2$(OAc)$_2$] (3).* The synthetic route for complex **3** was the same as that of **1**. Yield: 1.36 g (80%). Anal. Calcd for $C_{30}H_{44}Cu_2N_4O_6{\cdot}2H_2O$: N, 7.78; C, 50.06; H, 6.72%. Found: N, 7.80; C, 50.28; H, 6.27%. *m*/*z* (ESI-MS, DMSO): 623.3 ($[M-CH_3COO]^+$, 100%, calcd. 623.17). Characteristic IR absorptions (cm$^{-1}$, neat): 1606 ($\nu_{C=N}$), 1566 ($\nu_{\text{asymmetric acetate}}$), 1407 ($\nu_{\text{symmetric acetate}}$).

*Synthesis of Complex [($L^1$)$_2$Cu$_2$(OAc)$_2$] (4).* All manipulations for synthesis of compound **4** were carried out under a dry nitrogen atmosphere. A mixture of 2-{1-[2-(dimethylamino)ethyl)imino]-ethyl}-4-methylphenol (1.12 g, 5.1 mmol) and $Cu(OAc)_2$ (0.900 g, 5.0 mmol) was stirred in refluxing anhydrous methanol (30 mL) for 24 h. The solution was then cooled to room temperature. The solution was concentrated to ca. 5 mL, followed by filtration to yield blue solids. Yield: 1.28 g (75%). Anal. Calcd for $C_{30}H_{44}Cu_2N_4O_6{\cdot}2MeOH$: N, 7.49; C, 51.39; H, 7.01%. Found: N, 7.55; C, 51.34; H, 6.09%. *m*/*z* (ESI-MS, DMSO): 623.2 ($[M-CH_3COO]^+$, 100%, calcd. 623.2).

*Synthesis of Complex [($L^4$)$_2$Cu$_3$(OAc)$_4$] (5).* A mixture of 4-methoxy-2-{1-[2-(dimethylamino)ethylimino]ethyl}phenol (1.54 g, 4.1 mmol) and $Cu(OAc)_2{\cdot}H_2O$ (1.19 g, 6.0 mmol) was dissolved in ethanol (30 mL), and the solution was heated under reflux for 24 h. The solution was then cooled to room temperature. Volatile materials were removed to leave about 5 mL under vacuum to yield blue solids. The blue powder was obtained after filtration. Yield: 1.52 g (85%). Anal. Calcd for $C_{34}H_{50}Cu_3N_4O_{12}$: N, 6.24; C, 45.50; H, 5.62%. Found: N, 6.20; C, 45.70; H, 5.74%. *m*/*z* (ESI-MS, DMSO): 655.3 ($[M-Cu(OAc)_3]^+$, 100%, calcd. 655.13). Characteristic IR absorptions (cm$^{-1}$, neat): 1610 ($\nu_{C=N}$), 1589 ($\nu_{\text{asymmetric bridging bidentate acetate}}$), 1526 ($\nu_{\text{asymmetric monodentate acetate}}$), 1426 ($\nu_{\text{symmetric bridging bidentate acetate}}$), 1396 ($\nu_{\text{symmetric monodentate acetate}}$).

*Copolymerization of $CO_2$ and CHO Catalyzed by Complexes* **1**−**5**. A representative procedure for the copolymerization of cyclohexene oxide with $CO_2$ (Table 2, entry 8) was exemplified. Cu catalyst **3** (0.0682 g, 0.1 mmol) was dissolved in 5.0 mL of neat cyclohexene oxide under a dry nitrogen atmosphere. Under $CO_2$ atmosphere, the mixed solution was added to the 100 mL autoclave with magnetic stirrer. $CO_2$ was then charged into the reactor until the pressure of 300 psi was reached, and the stirrer was started. The reaction was performed at 120 °C for 48 h. Then the reactor was placed into ice water, and excess $CO_2$ was released. The CHO conversion (88%) was analyzed by $^1$H NMR spectroscopic studies. Spectral characteristics of cyclohexene carbonate: poly(cyclohexene carbonate) (PCHC) carbonate ($\delta$: 4.65 ppm), PCHC ether ($\delta$: 3.3−3.5 ppm), and CHC ($\delta$: 3.9 (trans) or 4.63 ppm (cis)). The mixture was diluted with $CH_2Cl_2$ (50 mL), followed by the addition of 1 N HCl solution (1.0 mL) to quench this reaction, and the final mixture was passed through a short column of neutral alumina to remove the metal salt. After precipitation by adding polymer solution in $CH_2Cl_2$ into methanol (50 mL) three times, the off-white polymer was collected by filtration and dried under vacuum overnight.

**X-ray Crystallographic Studies.** Single crystals of complexes **1**−**5** were obtained from their saturated ethanol or methanol solutions. Suitable crystals were immersed in FOMBLINY under nitrogen atmosphere and mounted on an Oxford Xcalibur Sapphire-3 CCD Gemini diffractometer employing graphite-monochromated Mo K$\alpha$ radiation ($\lambda$ = 0.710 73 Å), and intensity data were collected with $\omega$ scans. The data collection and reduction were performed with the CrysAlisPro software,[17] and the absorptions were corrected by the SCALE3 ABSPACK multiscan method.[18] The space-group determination was based on a check of the Laue symmetry and systematic absences, and it was confirmed using the structure solution. The structure was solved and refined with the SHELXTL package.[19] All non-H atoms were located from successive Fourier maps, and hydrogen atoms were refined using a riding model. Anisotropic thermal parameters were used for all non-H atoms, and fixed isotropic parameters were used for H atoms. Crystallographic data of complexes **1**−**5** are summarized in Supporting Information, Table S1.

## ■ ASSOCIATED CONTENT

### Ⓢ Supporting Information

Absorption spectra of complexes **1**−**5**, $^1$H NMR spectrum of copolymer selectivity by **3**, and crystallographic details. This material is available free of charge via the Internet at http://pubs.acs.org. CCDC 980348−980351 and −992731 (for **1**−**5**) contain the supplementary crystallographic data in this paper.

## AUTHOR INFORMATION

### Corresponding Authors

*E-mail: btko@dragon.nchu.edu.tw. Phone: 886-4-22840411-715. Fax: 886-4-22862547 (B.T.K.).

*E-mail: cchlin@mail.nchu.edu.tw. Phone: 886-4-22840411-718. Fax: 886-4-22862547 (C.C.L.).

### Notes

The authors declare no competing financial interest.

## ACKNOWLEDGMENTS

We gratefully acknowledge the financial support from the National Science Council, Taiwan (NSC101-2113-M-005-010-MY3 to C.C.L. and NSC101-2113-M-005-020-MY3 to B.T.K.).

## REFERENCES

(1) Inoue, S.; Koinuma, H.; Tsuruta, T. *J. Polym. Sci., Part B* **1969**, *7*, 287–292.

(2) (a) Coates, G. W.; Moore, D. R. *Angew. Chem., Int. Ed.* **2004**, *43*, 6618–6639. (b) Darensbourg, D. J. *Chem. Rev.* **2007**, *107*, 2388–2410. (c) Sakakura, T.; Kohno, K. *Chem. Commun.* **2009**, 1312–1330. (d) Kember, M. R.; Buchard, A.; Williams, C. K. *Chem. Commun.* **2010**, *47*, 141–163. (e) Decortes, A.; Castilla, A. M.; Kleij, A. W. *Angew. Chem., Int. Ed.* **2010**, *49*, 9822–9837. (f) Darensbourg, D. J. *Inorg. Chem.* **2010**, *49*, 10765–10780. (g) Lu, X.-B.; Darensbourg, D. J. *Chem. Soc. Rev.* **2012**, *41*, 1462–1484. (h) Lu, X.-B.; Ren, W.-M.; Wu, G.-P. *Acc. Chem. Res.* **2012**, *45*, 1721–1735 and references therein. (i) Nakano, K.; Kobayashi, K.; Nozaki, K. *J. Am. Chem. Soc.* **2011**, *133*, 10720–10723. (j) Kember, M. R.; Jutz, F.; Buchard, A.; White, A. J. P.; Williams, C. K. *Chem. Sci.* **2012**, *3*, 1245–1255. (k) Liu, Y.; Ren, W.-M.; Liu, J.; Lu, X.-B. *Angew. Chem., Int. Ed.* **2013**, *52*, 11594–11598. (l) Chatterjee, C.; Chisholm, M. H.; El-Khaldy, A.; McIntosh, R. D.; Miller, J. T.; Wu, T. *Inorg. Chem.* **2013**, *52*, 4547–4553. (m) Darensbourg, D. J.; Wilson, S. J. *Macromolecules* **2013**, *46*, 5929–5934. (n) Nakano, K.; Kobayashi, K.; Ohkawara, T.; Imoto, H.; Nozaki, K. *J. Am. Chem. Soc.* **2013**, *135*, 8456–8459.

(3) Kember, M. R.; White, A. J. P.; Williams, C. K. *Macromolecules* **2010**, *43*, 2291–2298.

(4) Buchard, A.; Kember, M. R.; Sandemanb, K. G.; Williams, C. K. *Chem. Commun.* **2011**, *47*, 212–214.

(5) (a) Kember, M. R.; Knight, P. D.; Reung, P. T. R.; Williams, C. K. *Angew. Chem., Int. Ed.* **2009**, *48*, 931–933. (b) Kember, M. R.; White, A. J. P.; Williams, C. K. *Inorg. Chem.* **2009**, *48*, 9535–9542.

(6) Kember, M. R.; Williams, C. K. *J. Am. Chem. Soc.* **2012**, *134*, 15676–15679.

(7) (a) Macias, E. E.; Ratnasamy, P.; Carreon, M. A. *Catal. Today* **2012**, *198*, 215–218. (b) Ulusoy, M.; Şahin, O.; Kilic, A.; Büyükgüngör, O. *Catal. Lett.* **2010**, *141*, 717–725.

(8) (a) Chen, H.-Y.; Tang, H.-Y.; Lin, C.-C. *Macromolecules* **2006**, *39*, 3745–3752. (b) Hung, W.-C.; Huang, Y.; Lin, C.-C. *J. Polym. Sci., Part A: Polym. Chem.* **2008**, *46*, 6466–6476. (c) Hung, W.-C.; Lin, C.-C. *Inorg. Chem.* **2009**, *48*, 728–734.

(9) (a) Mondal, N.; Saha, M. K.; Bag, B.; Mitra, S.; Rosair, G.; Fallah, M. S. El *Polyhedron* **2001**, *20*, 579–584. (b) Lin, C. S.; Lin, C. H.; Huang, J. H.; Ko, B. T. *Acta Crystallogr., Sect. E: Struct. Rep. Online* **2008**, *64*, m1434. (c) Biswas, C.; Drew, M. G. B.; Ruiz, E.; Estrader, M.; Diaz, C.; Ghosh, A. *Dalton Trans.* **2010**, *39*, 7474–7484.

(10) Nakamoto, K. *Infrared and Raman Spectra of Inorganic and Coordination Compounds, Theory and Applications in Inorganic Chemistry*, 5th ed.; John Wiley and Sons, Inc.: New York, 1997.

(11) Tümer, M. *Synth. React. Inorg. Met.-Org. Chem.* **2000**, *39*, 1139–1158.

(12) Addison, A. W.; Rao, T. N.; Reedijk, J.; Rijn, J. V.; Verschoor, G. C. *J. Chem. Soc., Dalton Trans.* **1984**, 1349–1356.

(13) Thakurta, J. C. S.; Rosair, G.; Tercero, J.; Fallah, M. S. El; Garribba, E.; Mitra, S. *Inorg. Chem.* **2008**, *47*, 6227–6235.

(14) (a) Darensbourg, D. J.; Mackiewicz, R. M. *J. Am. Chem. Soc.* **2005**, *127*, 14026–14038. (b) Cohen, C. T.; Chu, T.; Coates, G. W. *J. Am. Chem. Soc.* **2005**, *127*, 10869–10878. (c) Ren, W.-M.; Liu, Z. W.; Wen, Y. Q.; Zhang, R.; Lu, X.-B. *J. Am. Chem. Soc.* **2009**, *131*, 11509–11518. (d) Darensbourg, D. J.; Wu, G.-P. *Angew. Chem., Int. Ed.* **2013**, *52*, 10602–10606.

(15) Moore, D. R.; Cheng, M.; Lobkovsky, E. B.; Coates, G. W. *J. Am. Chem. Soc.* **2003**, *125*, 11911–11924.

(16) Villa, A. C.; Guastini, C.; Blech, P.; Floriani, C. *Dalton Trans.* **1990**, 3557–3561.

(17) *CrysAlisPro*, Version 1.171; Agilent Technologies: Santa Clara, CA, 2009.

(18) *CrysAlisPro SCALE3 ABSPACK*, a scaling algorithm for empirical absorption correction using spherical harmonics; Oxford Diffraction (Agilent Technologies): Santa Clara, CA, 2005.

(19) Sheldrick, G. M. *Acta Crystallogr.* **2008**, *A64*, 112–122.